16th World Conference on Earthquake, 16WCEE 2017
Santiago Chile, January 9th to 13th 2017
Paper N° 3940 (Abstract ID)
Registration Code: S-P1463220593

EVALUATION OF SEISMIC EARTH PRESSURE ACTING ON FOOTING EMBEDDED IN COHESIVE SOIL BASED ON CENTRIFUGE TESTS

S. Tamura[(1)], D. Odaka[(2)], H. Mano[(3)] and Y. Shamoto[(4)]

[(1)] *Associate Professor, Tokyo Institute of Technology, tamura@arch.titech.ac.jp*
[(2)] *Graduate student, Tokyo Institute of Technology*
[(3)] *Manager, Construction Technology Department, Shimizu Corporation, mano_h@shimz.co.jp*
[(4)] *Research Fellow, Institute of Technology, Shimizu Corporation, shamoto@shimz.co.jp*

Abstract

This paper presents centrifuge test results for the seismic earth pressure acting on a footing embedded in cohesive soil. To clarify the effects of clay cohesion on the seismic earth pressure at the active and passive sides, two dynamic centrifuge tests were performed on a footing model supported by 2 × 2 piles embedded in an oil-based clay layer overlying a dense sand deposit. The cohesive soils were oil-based clays with cohesion values of 35 and 60 kN/m^2. The study results indicate that the passive earth pressure of a clay can be estimated approximately based on Rankine's theory. The relative displacement needed for the earth thrust at the passive side to reach a peak value was approximately 4%–6% of the embedment depth. The earth thrust at the active side acted on the footing in the form of a tensile force during strong shakings. However, the active earth pressure of a clay cannot be estimated by Rankine's theory. The active earth pressure was smaller than the theoretical value probably because the ultimate extension force between the clay and footing was smaller than that caused by the failure of the clay, that is, the Mohr circle of the clay touched the Mohr–Coulomb failure envelope. The relative displacement needed for the earth thrust to reach the active state was approximately 1%–2% of the embedment depth.

Keywords: Seismic earth pressure; Clay; Active earth pressure; Embedment effect; Rankine's theory

1. Introduction

During earthquakes, the seismic earth pressure acting on the footing and basement of a building affects the shear force and bending moment of piles. The seismic earth pressure also affects the pile stress of a bridge structure. In general, during a small earthquake, the resultant force of earth pressure—the difference between the earth pressures at the active and passive sides—acts on a footing in the form of a reaction force transmitted from the superstructure and reduces the shear force at the pile head. In contrast, during a strong earthquake, the resultant force acts on a footing embedded in soft soil deposits in the form of an external force and increases the shear force at a pile head. The embedment effects can be estimated by the seismic deformation method considering the earth pressure, which is inherently nonlinear to the displacement between the soil and footing [1]. Therefore, the estimation of the earth pressure at any lateral displacement is important for the seismic performance–based design of pile foundations.

The relationship between displacement and earth pressure has been investigated by performing full-scale loading tests [2, 3, 4], lateral loading tests [5], large-scale shaking table tests [6], and centrifuge tests [7, 8]. The estimation of the theoretical earth pressure at any lateral displacement has been proposed by Zhang et al. [9] and Shamsabadi et al. [10]. Most of the previous studies have been conducted on sand deposits. Although a full-scale test of bridge abutment using clay backfill was reported by Romstad et al. [11], very little is known about the earth pressure of cohesive soils.

The present study aims to (1) measure the seismic earth pressure at the active and passive sides of a footing embedded in cohesive soils during earthquakes, (2) clarify the effects of clay cohesion on the earth pressure at the active and passive sides, and (3) investigate the nonlinearity of earth pressure with respect to the displacement between the soil and footing. For this purpose, two cases of dynamic centrifuge tests were performed on a footing–pile model in soft cohesive soil whose cohesion was varied. The earth pressure acting on the footing embedded in the cohesive soil during shakings was measured directly by plates and load cells.

2. Centrifuge Tests

2.1 Test cases and models

Two cases of dynamic centrifuge tests were performed on the geotechnical centrifuge at the Disaster Prevention Research Institute, Kyoto University. The centrifugal acceleration was 50 G. A footing–pile model was prepared in a laminar shear box whose inner dimensions were 450 mm (length, 22.5 m) × 150 mm (width, 7.5 m) × 300 mm (height, 15 m), as shown in Fig. 1 and Pic. 1. Models C35 and C60 were the same, except that the cohesions of the oil-based clay used in these models were different. Here and in later instances in the manuscript, the values in parenthesis indicate the measurements in the prototype scale.

The soil model consisted of a 130-mm-thick (6.5-m-thick) layer of a cohesive soil layer overlying a 150-mm-thick (7.5-m-thick) layer of dense Toyoura sand (D_r = 90%). We used an oil-based clay to create the cohesive soil layer. The oil-based clay is convenient for use in centrifuge tests because the consolidation process, which requires a long time, need not be performed on the clay. The cohesion of an oil-based clay depends on its temperature. To investigate the properties of the oil-based clay, consolidated undrained triaxial tests and unconfined compressive tests were performed at a constant temperature of 20 °C. The cohesion and internal friction angle of the clay estimated by the triaxial tests were 31 kN/m^2 and 1.0°, respectively. The cohesion of the oil-based clay estimated by the unconfined compressive tests was 29 kN/m^2. These results indicate that the cohesion of the oil-based clay can be estimated approximately by unconfined compressive tests. Centrifuge tests were performed on Models C35 and C60, both of which contained the same oil-based clay, in summer and winter, respectively. The temperature of the oil-based clay was monitored using thermopiles during the centrifuge tests. The cohesions of the oil-based clay for Models C35 and C60 estimated by unconfined compressive tests were 35 and 60 kN/m^2, respectively. The unit weight of the oil-based clay was 18.0 kN/m^3.

The pile model was made of 2 × 2 extra super duralumin bars, whose diameter was 10 mm (0.5 m) and length was 230 mm (11.5 m). The bending stiffness of the pile was 35.3 Nm^2 (28.6 MNm^2). The pile heads were rigidly linked to a base plate of the footing model, and their tips were also rigidly linked to a plate on the shear box base. The footing was 133 mm (6.65 m) in length, 106 mm (5.3 m) in width, and 60 mm (3 m) in height. The footing was embedded in the oil-based clay to a depth of 50 mm (2.5 m). The mass of the footing was 1.7 kg (213 ton). To measure the earth pressure acting on the footing, plates and load cells were set up at the left and right sides of the footing. The measurement system of the earth pressure is described in more detail by Tamura and Hida [1]. Sand papers with a grit size of 120 were set at the left and right sides of the footing, whereas Teflon sheets were set on the sidewalls of the footing to reduce the friction, considering that the distance between the footing and shear box wall was only 22 mm. The acceleration of the footing, soil, and shear box base and the strain of the piles were also measured. The input motion was "Rinkai92," which is a synthesized ground motion for the Tokyo Bay area. The maximum input accelerations, a_{max}, were scaled from 0.5 to 8.0 m/s^2 in the prototype scale. All the test results are presented in the prototype scale.

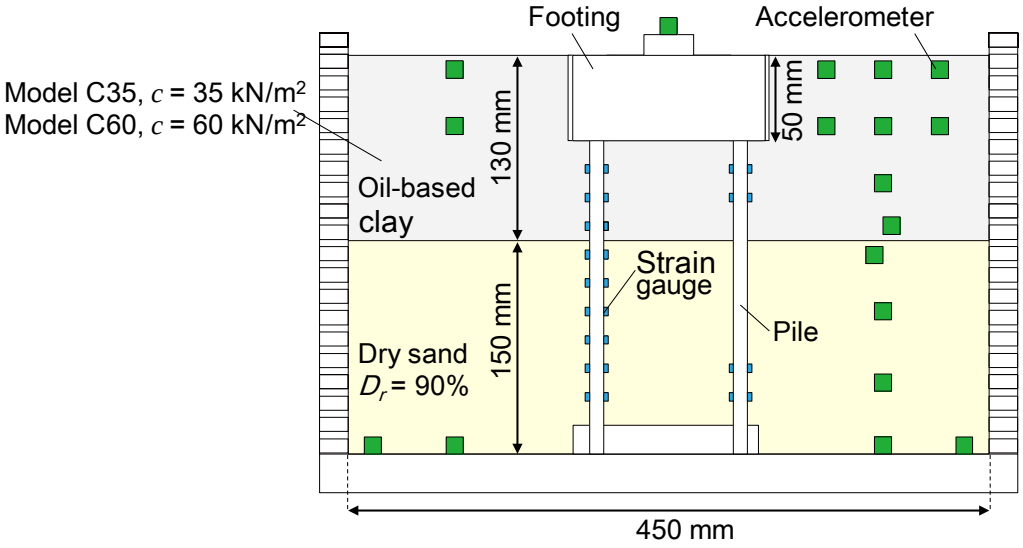

Fig. 1 – Test models

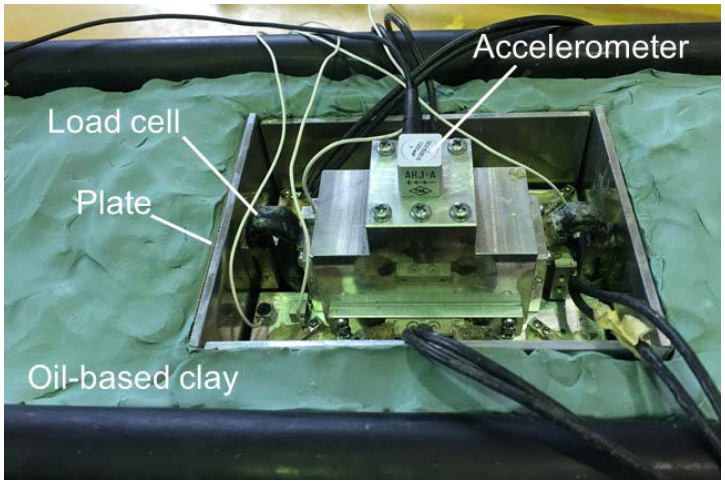

Pic. 1 – Footing and oil-based clay

2.2 Centrifuge test results

2.2.1 Test results for shaking at a_{max} = 2 m/s^2

The time histories of the acceleration of the shear box base, ground surface, top of the footing; displacement of the ground surface and footing; and earth thrust at the left side of the footing for a shaking at a_{max} = 2 m/s^2 are shown in Figs. 2 and 3. The earth thrust—the earth pressure acting on a plate—was measured directly by a load cell set on the footing. The amplitudes of the ground surface acceleration were slightly larger than those of the input motions for both the test cases. The earth pressure amplitude before the shaking was approximately 0.3 MN, so that the earth pressure coefficient at rest was approximately 1 for both the cases. The earth thrust was defined to be at the active and passive sides when the earth thrust amplitude during shaking was smaller and larger than that at rest, respectively. The earth thrust during shakings at the active and passive sides had almost the same amplitudes, approximately 0.3–0.4 MN. Most of the earth thrust peaks were positive, that is, compressive forces. The amplitudes of the ground surface and footing displacement for Model C35 were apparently larger than those for Model C60. On the other hand, the amplitudes of the earth thrust for Model C35 were smaller than those for Model C60, suggesting that clay cohesion affected the soil displacement and earth pressure.

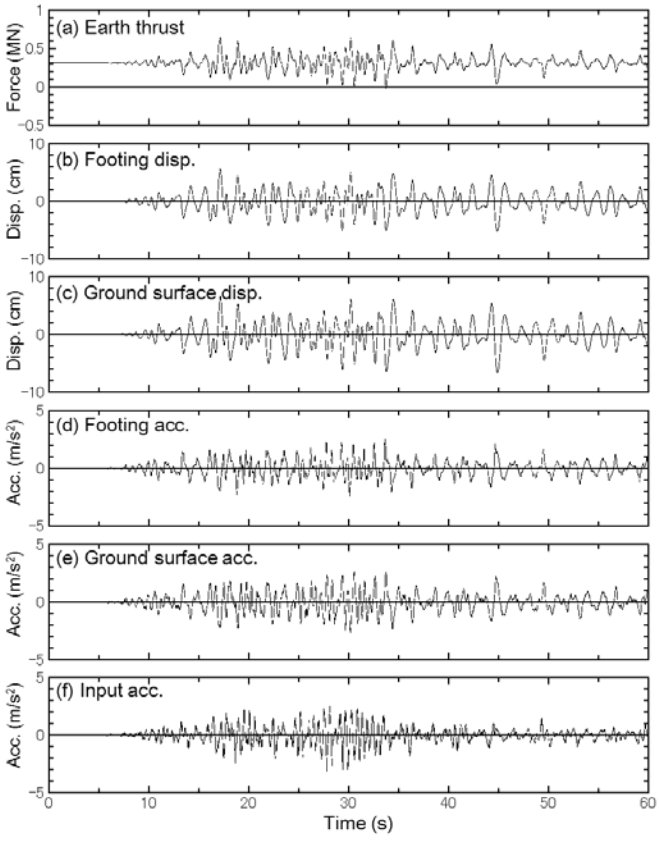

Fig. 2 – Test results for Model C35 (a_{max} = 2 m/s^2)

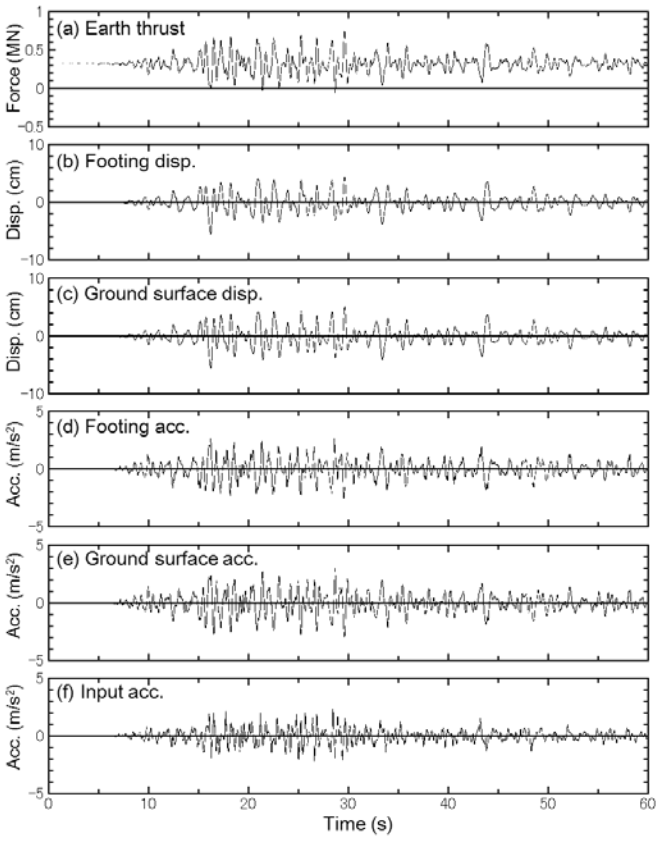

Fig. 3 – Test results for Model C60 (a_{max} = 2 m/s^2)

2.2.2 Test results for shaking at a_{max} = 8 m/s^2

The time histories of the measured data for strong shaking at a_{max} = 8 m/s^2 for Models C35 and C60 are shown in Figs. 4 and 5, respectively. The predominant periods of the ground surface acceleration were longer than those of the input motions for both the models. The footing acceleration contained short-period components, suggesting that the seismic wave propagated from the shear box base to the footing through the piles. The amplitude of the ground surface displacement for Model C35 tended to be larger than that for Model C60, but the amplitude of the earth thrust for Model C35 was apparently smaller than that for Model C60. The earth thrust amplitudes at the active side were clearly smaller than those at the passive side for both the models. Moreover, some peaks of the earth thrust at the active side were negative, indicating that the earth pressure acted on the footing in the form of a tensile force.

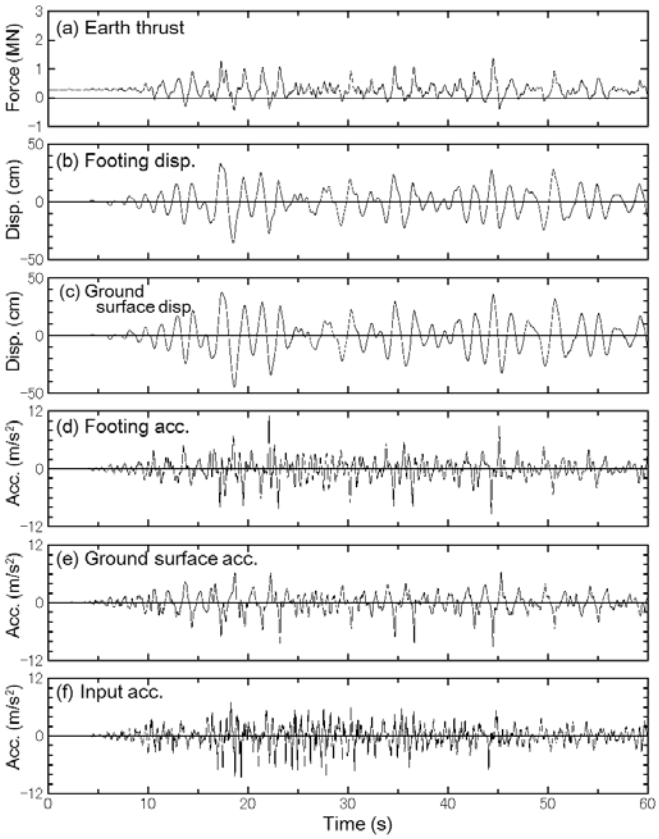

Fig. 4 – Test results for Model C35 (a_{max} = 8 m/s^2)

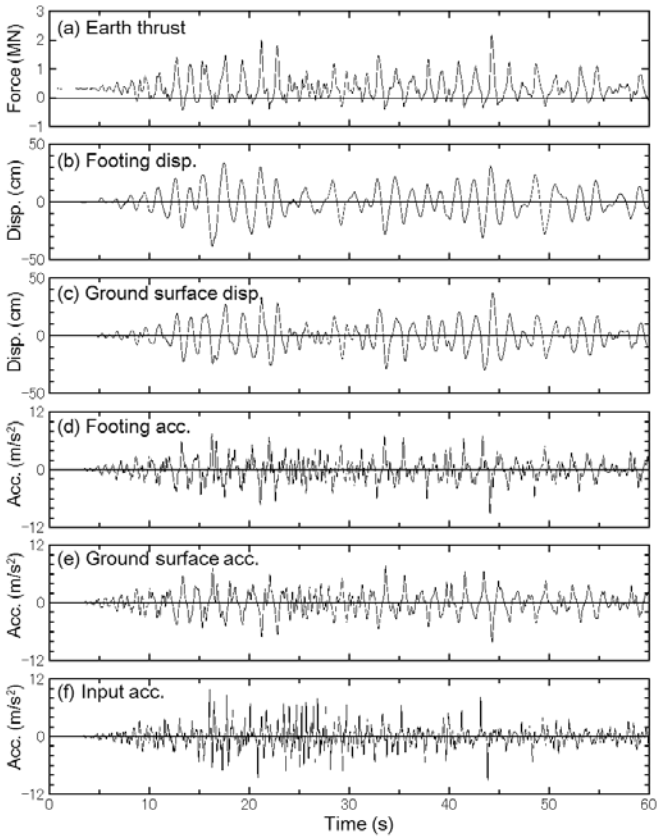

Fig. 5 – Test results for Model C60 (a_{max} = 8 m/s^2)

The hysteresis loops of the relative displacement and earth thrust acting on the left and right sides of the footing for a strong shaking at a_{max} = 8 m/s^2 are shown in Figs. 6 and 7. The relative displacement was observed between the footing and soil at the middle of the footing's embedment depth. The amplitude of the earth thrust at the passive side tended to increase as the relative displacement increased for both the models. In contrast, the amplitude of the earth thrust at the active side tended to be constant, although the relative displacement amplitude increased. The earth thrust amplitudes at the passive side for Model C60 were clearly larger than those for Model C35 in spite of a smaller relative displacement. It is interesting to note that the earth thrust amplitudes at the active side for Model C60 were almost the same as those for Model C60. These results suggest that the passive earth pressure of a clay depends on its cohesion but that the active earth pressure does not depend on its cohesion. The hysteresis loops at the left and right sides had similar tendencies, and therefore, we hereafter discuss the earth thrust measured at the left side of the footing.

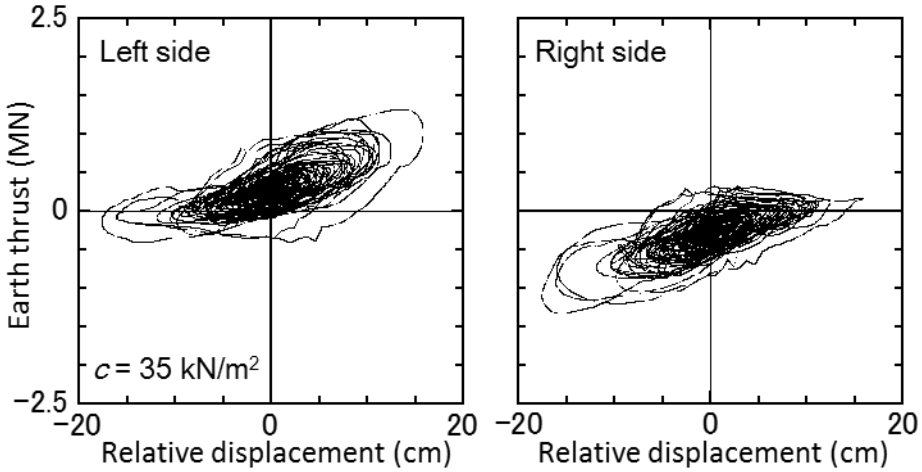

Fig. 6 – Relative displacement and earth thrust for Model C35 (a_{max} = 8 m/s^2)

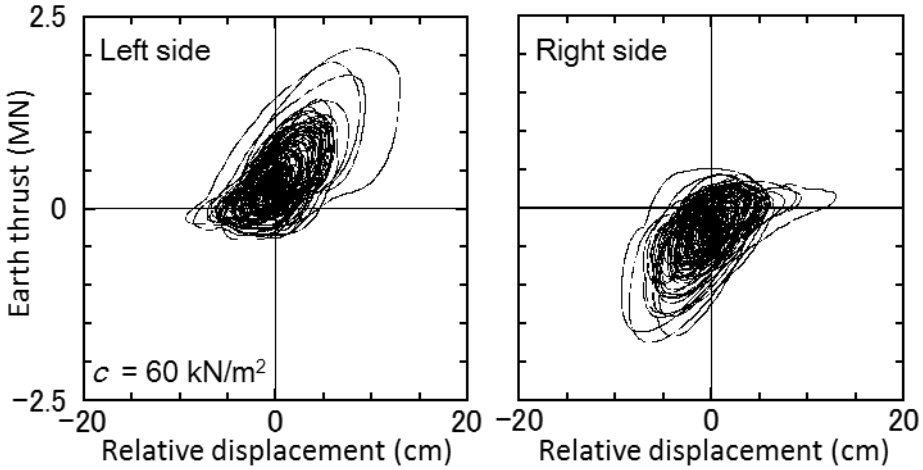

Fig. 7 – Relative displacement and earth thrust for Model C60 (a_{max} = 8 m/s^2)

3. Seismic Earth Pressure of Clay and Rankine's theory

To evaluate the seismic earth pressure quantitatively, the earth pressure coefficients are discussed according to Rankine's theory, which is a widely accepted earth pressure theory. The measured earth pressure coefficient K_m is estimated as follows:

$$K_m = \frac{P_m}{\frac{1}{2}\gamma B H^2} \tag{1}$$

where P_m is the measured earth thrust acting on the left or right side of the footing, γ is the unit weight of the soil, H is the depth of the embedded footing, and B is the width of the footing. The positive and negative coefficients represent the compression and tension forces, respectively. The relationship between the relative displacement and earth pressure coefficients at the left side of the footing for shakings at a_{max} = 2–8 m/s^2 is shown in Fig. 8. The relative displacement D_{re} was divided by the footing depth H. D_{re}/H increased as the input acceleration increased. Hysteresis loops were elliptical in shape for the shaking at a_{max} = 2 m/s^2. The amplitude of the earth thrust at the passive and active sides increased linearly as D_{re}/H increased. Therefore, the earth thrusts during the shakings at the active and passive sides had almost the same amplitudes, as shown in Fig. 2. When the input acceleration was a_{max} = 4 m/s^2, the hysteresis loop for Model C60 was elliptical in shape but that for Model C35 had a slightly different shape. The hysteresis loop shapes markedly varied for strong shakings (a_{max} = 6 and 8 m/s^2). As the relative displacement increased, the amplitude of the earth thrust at the passive side increased but that at the active side tended to remain constant.

The theoretical active and passive earth pressures based on Rankine's theory are also shown in Fig. 8. The active earth pressure coefficient K_a and passive earth pressure coefficient K_p are estimated as follows:

$$K_a = \frac{P_a}{\frac{1}{2}\gamma H^2} \tag{2}$$

$$K_p = \frac{P_p}{\frac{1}{2}\gamma H^2} \tag{3}$$

$$P_a = \int_0^H (\gamma z - 2c)\,dz = \frac{1}{2}\gamma H^2 - 2cH \tag{4}$$

$$P_p = \int_0^H (\gamma z + 2c)\,dz = \frac{1}{2}\gamma H^2 + 2cH \tag{5}$$

where P_a is the active earth pressure, P_p is the passive earth pressure, and c is the cohesion of clay. The estimated earth pressure coefficients in the passive state were 4.1 for Model C35 and 6.3 for Model C60. The maximum amplitudes of the measured earth pressure in the form of a compressive force were slightly larger than Rankine's passive earth pressure for a strong shaking at a_{max} = 8 m/s^2. On the other hand, the estimated earth pressure coefficients in the active state were -2.1 for Model C35 and -4.4 for Model C60. The minus sign shows that the earth thrust acted on the footing in the form of a tensile force. The maximum amplitudes of the earth pressure were much smaller than Rankine's active earth pressure for both the models. This fact suggests that the passive earth pressure of a clay can be estimated approximately based on Rankine's theory. However, the active earth pressure of a clay cannot be estimated by Rankine's theory. The active earth pressure was smaller than the theoretical value probably because the ultimate extension force between the clay and footing was smaller than that caused by the failure of the clay, that is, the Mohr circle of the clay touched the Mohr–Coulomb failure envelope.

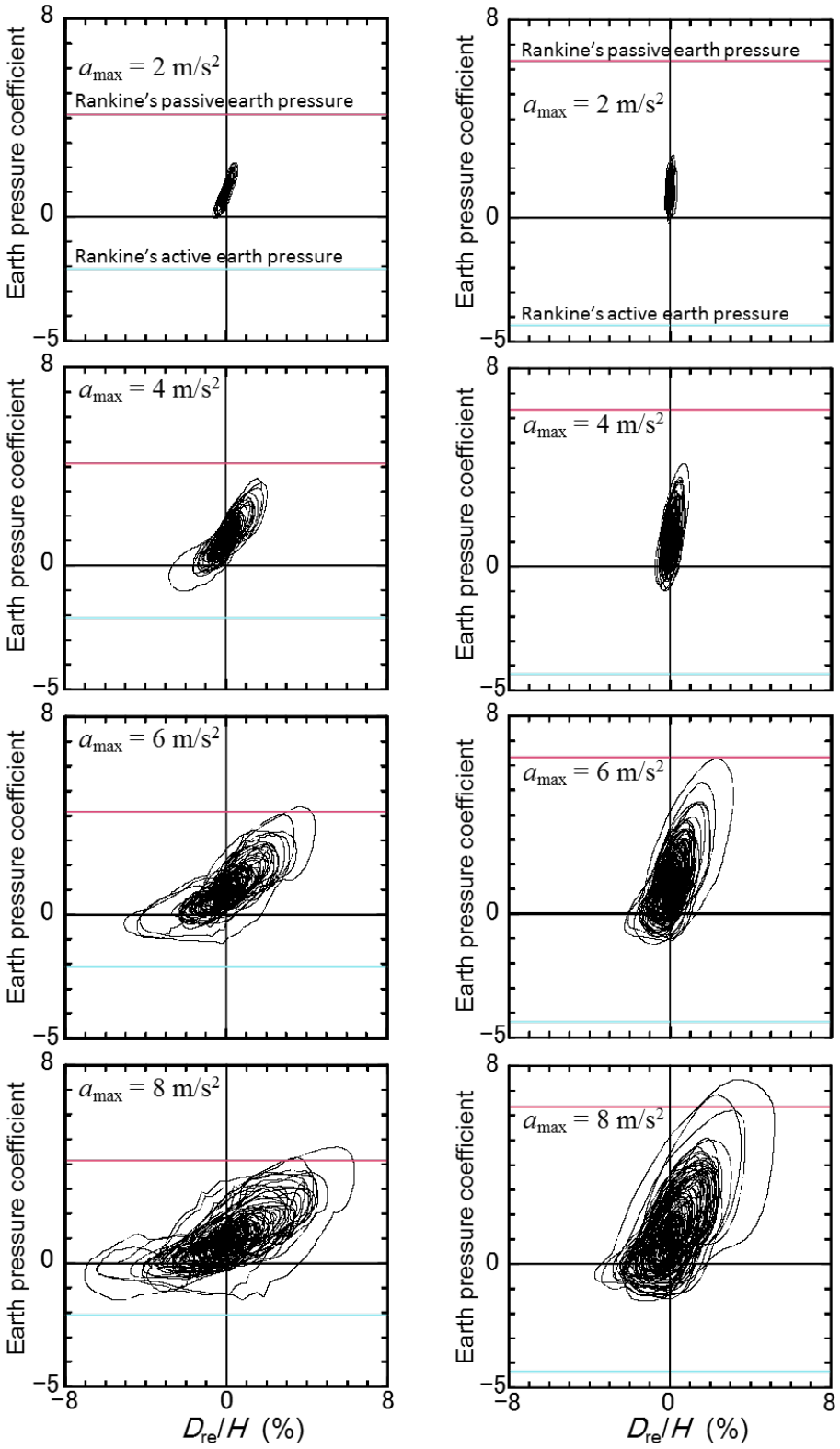

(a) Model C35 (b) Model C60

Fig. 8 – Relative displacement and earth pressure coefficients for Models C35 and C60 (a_{max} = 2–8 m/s^2)

To estimate the seismic earth pressure at any lateral displacement, determining the relative displacements D_{re}/H required to reach the active and passive states is important. The variation in the measured earth pressure coefficient peaks at the passive side that are larger than the previous values for each shaking is shown in Fig. 9. The earth pressure coefficient peaks increased as D_{re}/H increased. For both the models, the relationship between D_{re}/H and the earth pressure peaks showed similar trends in spite of different input accelerations being used. The measured maximum earth pressure coefficients were 4.8 for Model C35 and 7.5 for Model C60. The relationship between D_{re}/H and the earth thrust suggested that the maximum earth thrusts almost reached the passive state. The relative displacement needed for the earth thrust at the passive side to reach a peak value was approximately D_{re}/H = 4%–6%. The D_{re}/H range was almost the same as that for a sand deposit reported by Zhang et al. [9] and Shamsabadi et al. [10]. The peak values were slightly larger than Rankine's passive earth pressure.

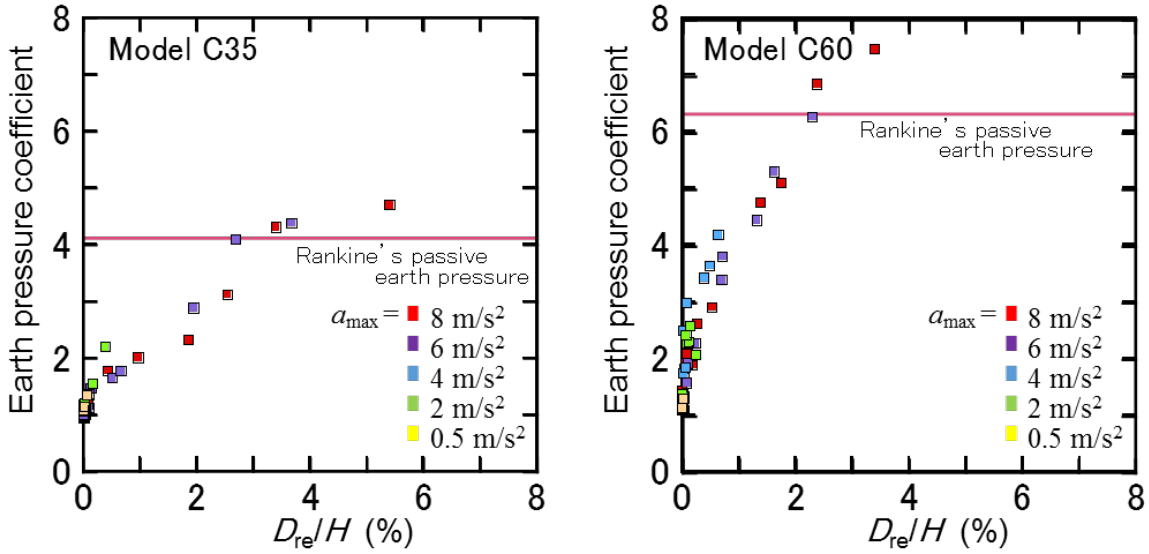

Fig. 9 – Relative displacement and earth pressure coefficient peaks at passive side for Models C35 and C60 (a_{max} = 0.5–8 m/s^2)

Figure 10 shows the variation in the measured earth pressure coefficient peaks at the active side that are smaller than the previous values. The earth pressure coefficient peaks at the active side became negative when D_{re}/H was extremely small. The earth pressure coefficient peaks seemed to increase as D_{re}/H increased. The measured earth pressure coefficient peaks at the active side, which were -1.5 for both the models, were clearly smaller than those estimated using Rankine's active earth pressure, i.e., -2.1 for Model C35 and -4.4 for Model C60. The peak earth thrust was inferred to have reached the active state because the amplitude of the earth thrust at the active side tended to be constant as the relative displacement amplitude increased, as shown in Fig. 8. The relative displacement needed for the earth thrust to reach the active state was approximately D_{re}/H = 1%–2%. D_{re}/H obtained here was larger than that for a sand deposit reported by Zhang et al. [9].

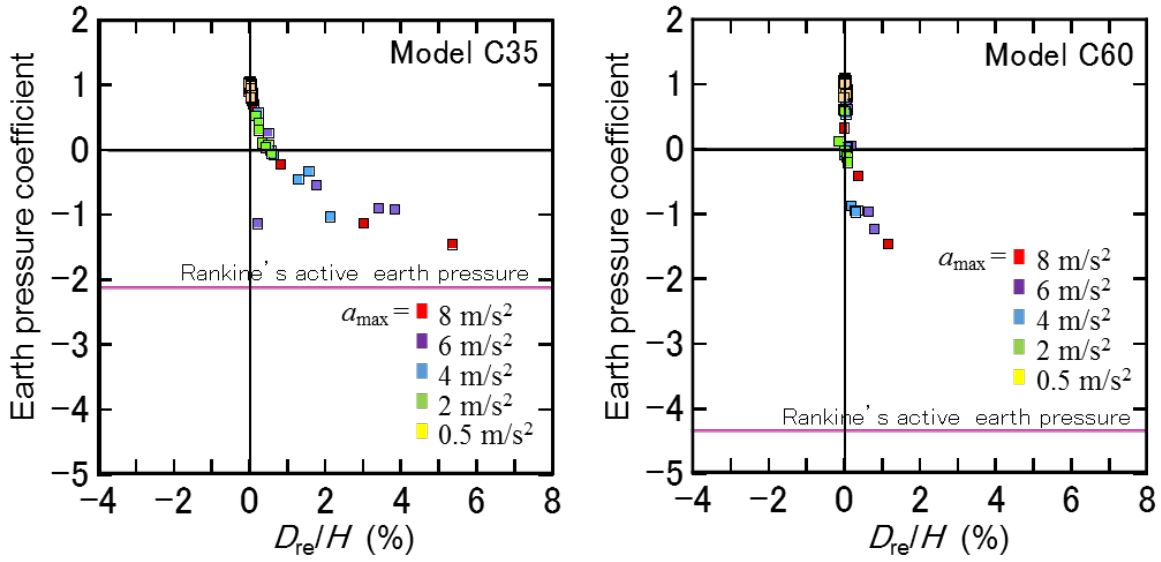

Fig. 10 – Relative displacement and earth pressure coefficient peaks at active side for Models C35 and C60 (a_{max} = 0.5–8 m/s^2)

4. Conclusions

In this study, to clarify the seismic earth pressure of cohesive soils, two dynamic centrifuge tests were performed on a footing–pile model in soft cohesive soil whose cohesion was varied. The cohesive soils were oil-based clays with cohesion values of 35 and 60 kN/m^2. The following conclusions were drawn from the results of the study:

1) When the input acceleration amplitudes were smaller than approximately 2 m/s^2, the amplitudes of the earth thrust at the passive and active sides increased as the relative displacement between the footing and soil increased. Most of the earth pressure acted on the embedded footing in the form of a compressive force even at the active side. When the input accelerations were strong (a_{max} = 6 and 8 m/s^2) and as the relative displacement increased, the amplitudes of the earth thrust at the passive side increased but those at the active side tended to remain constant and acted on the footing in the form of a tensile force.
2) The maximum earth pressure coefficients at the passive side were 4.8 for Model C35 (the cohesion of the clay was 35 kN/m^2) and 7.5 for Model C60 (the cohesion of the clay was 60 kN/m^2). The peak values were slightly larger than Rankine's passive earth pressure. The passive earth pressure of a clay can be estimated approximately based on Rankine's theory. The relative displacement needed for the earth thrust at the passive side to reach a peak value was approximately 4%–6% of the embedment depth.
3) The maximum earth pressure coefficients at the active side were approximately 1.5 for both the models (Models C35 and C60) regardless of the cohesion of the clay. The peak values were apparently smaller than Rankine's active earth pressure; nevertheless, the peak earth thrust was inferred to have reached the active state because the amplitude of the earth thrust at the active side tended to be constant as the relative displacement amplitude increased. The measured earth thrust amplitudes were smaller than those estimated by Rankine's theory probably because the ultimate extension force between the clay and footing was smaller than that caused by the failure of the clay. The relative displacement needed for the earth thrust to reach the active state was approximately 1%–2% of the embedment depth.

The results of the centrifuge tests show that the seismic earth pressure of a clay, especially at the active side, is different from that of a sand deposit. This study used an oil-based clay as the cohesive soil. Therefore, it might be possible that the test results do not adequately represent the behavior of cohesive soil. Further studies are

needed to evaluate the embedment effects of a footing in cohesive soil, including the validity of using the oil-based clay.

5. References

[1] Tamura S, Hida T (2014): Pile stress estimation based on seismic deformation method with embedment effects on pile caps. *Journal of Geotechnical and Geoenvironmental Engineering*, **140** (9), 04014049.

[2] Mokwa RL, Duncan JM (2001): Experimental evaluation of lateral-load resistance of pile caps. *Journal of Geotechnical and Geoenvironmental Engineering*, **127** (2), 185-192.

[3] Rollins KM, Sparks A (2002): Lateral resistance of full-scale pile cap with gravel backfill. *Journal of Geotechnical and Geoenvironmental Engineering*, **128** (9), 711-723.

[4] Rollins KM, Cole RT (2006): Cyclic lateral load behavior of a pile cap and backfill. *Journal of Geotechnical and Geoenvironmental Engineering*, **132** (9), 1143-1153.

[5] Fang YS, Ho YC, Chen TJ (2002): Passive earth pressure with critical state concept. *Journal of Geotechnical and Geoenvironmental Engineering*, **128** (8), 651-659.

[6] Tamura S, Tokimatsu K (2006): Seismic earth pressure acting on embedded footing based on large-scale shaking table tests. In *Seismic Performance and Simulation of Pile Foundations in Liquefied and Laterally Spreading Ground* (pp. 83-96). ASCE.

[7] Gadre A, Dobry R (1998): Lateral cyclic loading centrifuge tests on square embedded footing. *Journal of Geotechnical and Geoenvironmental Engineering*, **124** (11), 1128-1138.

[8] Tamura S, Imayoshi T, Sakamoto T (2007): Earth pressure and sidewall friction acting on an embedded footing in dry sand based on centrifuge tests. *Soils and Foundations*, **47** (4), 811-819.

[9] Zhang J-M, Shamoto Y, Tokimatsu K (1998): Evaluation of earth pressure under any lateral deformation. *Soils and Foundations*, **38** (1), 15-33.

[10] Shamsabadi A, Rollins KM, Kapuskar M (2007): Nonlinear soil–abutment–bridge structure interaction for seismic performance-based design. *Journal of Geotechnical and Geoenvironmental Engineering*, **133** (6), 707-720.

[11] Romstad K, Kutter B, Maroney B, Vanderbilt E, Griggs M, Chai YH (1995): Experimental measurements of bridge abutment behavior. *Report No. UCD-STR-95-1*, Department of Civil and Environmental Engineering, University of California, Davis, California.